International Journal of Environmental Sciences
ISSN: 2229-7359
Vol. 11 No.9s, 2025
https://www.theaspd.com/ijes.php

Glucose-Insulin Control System Impacted By Time and Spatial Variations in Carbohydrate Intestinal Absorption: Analytical Solution and Analysis of Integro-Differential Model

Jeerawan Suksamran[1], Yongwimon Lenbury[2,3]*, Chontita Rattanakul[2,3] and Pairote Satiracoo[2,3]
[1]Department of Mathematics, King Mongkut's University of Technology North Bangkok, Bangkok 10800, Thailand
[2]Department of Mathematics, Faculty of Science, Mahidol University, Bangkok 10400, Thailand
[3]Centre of Excellence in Mathematics, PERDO, MHESI, Bangkok, Thailand
*Corresponding Author: scylb@yahoo.com

Abstract: *Together with protein and fat, carbohydrates are among the macronutrients in the human diet, playing an important role in the anatomy. The process of breaking down carbohydrates into glucose begins in the digestive tract. Glucose is absorbed across the membrane of the small intestine and conveyed to the liver where they are either utilized, or distributed to the more remote parts of the human body. Sugar levels in the bloodstream then increase, triggering secretion of insulin which motivates the body's cells to absorb glucose for energy. High carbohydrates consumption may contribute to obesity, cardiovascular diseases, and type 2 diabetes. However, it was reported that "the risk of developing type 2 diabetes is lowered as the amount of calories from carbohydrates is increased. Diet that are high in carbohydrates tend to increase the sensitivity of insulin." Nowadays, some healthcare providers routinely recommend high carbohydrate diet to type 2 diabetics, whose risk of heart disease has been observed to lower. To investigate this paradoxical effects, we construct a 3 compartmental dynamical model of the glucose-insulin control system incorporating the carbohydrate absorption process, described by an exponential function so that the amount absorbed per unit of digested carbohydrate varies with space and time. We arrive at an integro-differential system model, which is analyzed for its stability. Its analytical solution obtained as a traveling wave solution, and the time series of glucose and insulin levels provide valuable insights into the impacts of starch content on the glucose-insulin control system for diabetics or healthy subjects.*

Keywords: *Carbohydrate absorption, glucose-insulin control system, integro-differential model equations, stability analysis, traveling wave solutions, type 2 diabetes*

INTRODUCTION

In addition to protein and fat in the human diet, carbohydrates are known to be among the macronutrients which play a crucial role in the proper function of the human anatomy [1]. The beginning of the process of breaking down carbohydrates into glucose begins in the digestive tract upon consumption, yielding energy. Glucose, fructose, and galactose are absorbed across the membrane of the small intestine and conveyed to the liver where they are either utilized by the liver, or distributed to the more remote parts of the human body. Any remaining glucose in circulation is stored in the liver and muscle tissue until additional energy is required. As carbohydrates are digested, the sugar levels in the bloodstream increase, triggering insulin secretion by the pancreas. Insulin then motivates the body's cells to absorb glucose for energy. Any extra glucose in the bloodstream is stored in the liver and muscle tissue until further energy is needed. According to [1], the term *Carbohydrates* is an umbrella term that includes sugar, fruits, vegetables, encompassing fibres, and legumes. Although they may be delineated into many divisions, benefits to human are mostly derived from only a certain subset of these [2, 3].

A diet needs to be nutritionally balanced, consisting the proper amount of carbohydrates. A rise or fall of carbohydrate levels beyond the appropriate amount can impact both physiological and metabolic activities. High carbohydrates may contribute to obesity, leading to cardiovascular diseases. Several investigations reported that carbohydrate intake can also contribute to type 2 diabetes. In addition,

foods rich in non-starch polysaccharides and low-glycemic foods protect against diabetes, among other illnesses. On the other hand, according to [1], data have been reported that show that "the risk of developing type 2 diabetes is lowered as the amount of calories from carbohydrates is increased. Diet that are high in carbohydrates tend to increase the sensitivity of insulin." Therefore, nowadays, some healthcare providers routinely recommend high carbohydrate diet to type 2 diabetics, whose risk of heart disease has been observed to lower.

To investigate this paradoxical effects, we construct a 3 compartmental dynamical model of the glucose-insulin control system which incorporates the process of carbohydrate absorption in the small intestine. The model tracks the changes in the levels of glucose and insulin which are effected by the level of carbohydrates, the cross-membrane absorption process being described by an exponential function so that the amount absorbed per unit of digested carbohydrate varies with space and time. Thus, the rate of change of the amount of carbohydrates is modeled by a partial differential equation. We accordingly arrive at a dynamical model consisting of a system of integro-differential non-autonomous equations.

After the introduction of new state variables which vary with the traveling wave coordinate, the model can be transformed into an autonomous system of ordinary differential equations. Stability analysis is carried out to discover the dynamical behavior of the solution near the system's equilibrium state. Analytical solution is subsequently obtained in the form of a wave solution traveling along the length of the digestive tract. The resulting simulated graphs of glucose and insulin levels as functions of time provide valuable insights and shed light on the impacts of high or low starch content in our food intake on the glucose-insulin control system for diabetics or healthy subjects.

METHODS

Model System

To better understand how carbohydrates upon consumption and the process of cross membrane absorption may impact the dynamics of glucose levels in the blood stream and the control mechanism in the human anatomy involving insulin secretion by the pancreas, we let

$C(t,\ z) = \text{carbohydrate content},$

$G(t) = \text{glucose concentration},$

$I(t) = \text{insulin concentration},$

where t denotes the time, and x denotes the spatial radial distance measured from a point of reference at the surface of the small intestine. Extending the models considered in [4] and [5] to incorporate carbohydrate absorption prose, we then arrive at the following model equations.

$$\frac{\partial C}{\partial t} = k_{CC}\frac{\partial C}{\partial z} + D\frac{\partial^2 C}{\partial z^2} - k_{GC}(z,t)C, C(0,z) = C_0 > 0, \tag{1}$$

$$\frac{dG}{dt} = R_0 + \int_0^l k_{GC}(z)C(t,z)dz - GS_I\frac{I}{I_{GS_0} + I}, G(t_0) = G_0 \ > 0, \tag{2}$$

$$\frac{dI}{dt} = \sigma^{\max}\frac{G^{\sigma_{IG}}}{G_{IS_0}^{\sigma_{IG}} + G^{\sigma_{IG}}} - k_{0I}I, I(t_0) = I_0 \ > 0. \tag{3}$$

The first term on the right of (1) represents the rate of change of C due to active transport, with transport coefficient k_{CC}. The second term is the rate of change of C due to diffusion, with diffusion coefficient D, while the last term is the rate of its removal due to intestinal absorption, with the specific removal rate k_{CG} which is written as

$$k_{GC}(z,t) = \alpha e^{k_0(z-vt)}, \tag{4}$$

where v is the speed at which the digested carbohydrate moves along the intestine. When z equals vt, the rate of carbohydrate absorption per unit of carbohydrates present will be at the value a. The more time passes the term z – vt becomes more negative, and the less absorption should be possible due to saturation. This absorbed amount of carbohydrates leads to the increase in the rate of change of glucose in (2), the total amount of which needs to be the integral sum of kCG(z,t)C(t, z) over the length *l* of the intestine, namely the second term in (2). Thus, the first term on the right of (2) represents the rate of increase of glucose level at zero consumption, the second term is the rate of change of G due to carbohydrate consumption and subsequent absorption, and the last term gives the rate of decrease of G due to insulin which has been secreted by the pancreas triggered by the rise of glucose level in the bloodstream. Finally, in (3), the first term on the right represents the rate of increase of insulin due to the presence of glucose, while the last term is the removal rate by natural means, with specific removal rate k_{0I}.

In the next section, we shall analyse the model system (1) – (3) in order determine whether there exist some conditions under which the solution to our model remains close to, or tends asymptotically, to some steady state value. To this end, we introduce the traveling wave coordinate:

$\xi = x - ct$,

and the following new state variables as functions of ξ.

$$c(\xi) = c(z - vt) = C(t, z), \kappa(\xi) = \kappa(z - vt) = e^{k_0(z - vt)}$$

Stability Analysis

Letting

$$x = c(\xi), y = c'(\xi), w = \kappa(\xi), \tag{5}$$

where $(\ )'$ denotes the derivative with respect to $\xi = z - vt$, equation (1) becomes

$$-vc' = k_{cc}c' + Dc'' - \alpha\kappa c . \tag{6}$$

Using (5), (6) can be written as

$$-vy = k_{cc}y + Dy' - \alpha wc$$

which leads to

$$y' = \frac{\alpha}{D}wx - \frac{v + k_{cc}}{D}y \ .$$

Thus, we are led to the following system of autonomous ordinary differential equations.

$$x' = y \tag{7}$$

$$y' = \frac{\alpha}{D}wx - \frac{v + k_{cc}}{D}y \tag{8}$$

$$w' = k_0 w \tag{9}$$

To discover the stability behaviour of the system near the washout steady state $S = (0,0,0)$, at which point the right hand sides of (7) – (9) are zero, we find the Jacobian matrix of the model system about *S* to be

$$J(0,0,0)=\begin{pmatrix}0 & 1 & 0\\ 0 & -\frac{v+k_{cc}}{D} & 0\\ 0 & 0 & k_0\end{pmatrix} \tag{10}$$

$$\upsilon_1 = 0, \tag{11}$$

$$\upsilon_2 = -\frac{v+k_{cc}}{D} < 0, \tag{12}$$

and

$$\upsilon_3 = k_0 > 0. \tag{13}$$

Since one of the eigenvalues is zero, *S* is a non-hyperbolic equilibrium point, and its local stability cannot be determined by approximating the system by linearizing it. The non-linear terms have to be considered as well. Therefore, inspection of the considering (9) and the non-linear term in (8), we see that the system (7) – (9) is dynamically unstable in the (*x*, *y*, *w*)-space unless k_0 is negative.

In the next section, we derive the analytical solution to the model system in the form of traveling wave fronts by utilizing the extended hyperbolic tangent method based on the work of Taghizadeh and Mirzazadeh [6].

TRAVELING WAVE FRONTS

In this section, we shall employ the modified extended tanh method [6] to derive analytical solutions in terms of the traveling wave coordinate $\xi = x - vt$. This method has been made used of by several researchers [7, 8, 9, 10] concerning important phenomena of great interest, yielding insightful and valuable conclusions. The authors refer the readers to these research articles for its description, and detailed development as well as its various applications.

Analytical Solution

We attempt to find the solution of the system (7) – (9) by expressing the state variables as finite series of hyperbolic tangent functions in the form

$$x = \sum_{k=0}^{K} a_k \phi^k, \tag{14}$$

$$y = \sum_{l=0}^{L} b_l \phi^l, \tag{15}$$

$$w = \sum_{m=0}^{M} c_m \phi^m. \tag{16}$$

where $a_k, b_l,$ and c_m are constants, and $\phi(\xi) = \tanh(\mu\xi)$ satisfies the Riccati equation

$$\phi' = \mu\left(1-\phi^2\right). \tag{17}$$

We determine the values of K, L and M by first equating the highest order of ϕ in the linear term x' with the highest order of ϕ in the nonlinear term y in equation (7) which gives

$$K+1 = L. \tag{18}$$

Equating the highest order of ϕ in the linear term y' with the highest order of ϕ in the nonlinear term wx in equation (8) gives

$$L+1=K+M. \tag{19}$$

So, we obtain

$$K=2, L=3 \text{ and } M=2. \tag{20}$$

Substituting (20) into (14) – (16) we obtain

$$x(\phi)=a_0+a_1\phi+a_2\phi^2 \tag{21}$$

$$y(\phi)=b_0+b_1\phi+b_2\phi^2+b_3\phi^3 \tag{22}$$

$$w(\phi)=c_0+c_1\phi+c_2\phi^2 \tag{23}$$

Substituting $\phi=\tanh(\mu\xi)$ and the Riccati equation in equations (7) – (9), with the aid of (21) – (23), and equating the coefficients of each power of ϕ, we obtain a system of algebraic equations of the parameters $a_0, a_1, a_2, b_0, b_1, b_2, b_3, c_0, c_1,$ and c_2;

$$2a_2\mu+b_3=0,\ \ b_2+a_1\mu=0,\ \ b_1-2a_2\mu=0,\ \ b_0-a_1\mu=0,$$

$$\frac{\alpha}{D}a_2c_2+3b_3\mu=0,\ \ \frac{\alpha}{D}a_2c_1+\frac{\alpha}{D}a_1c_2+2b_2\mu-\frac{v+k_{cc}}{D}b_3=0,$$

$$\frac{\alpha}{D}a_2c_1+\frac{\alpha}{D}a_1c_2+2b_2\mu-\frac{v+k_{cc}}{D}b_3=0,\ \ \frac{\alpha}{D}a_2c_0+\frac{\alpha}{D}a_1c_1+\frac{\alpha}{D}a_0c_2-\frac{v+k_{cc}}{D}b_2+b_1\mu-3b_3\mu=0, \tag{24}$$

$$\frac{\alpha}{D}a_1c_0+\frac{\alpha}{D}a_0c_1-\frac{v+k_{cc}}{D}b_1-2b_2\mu=0,\ \ \frac{\alpha}{D}a_0c_0-\frac{v+k_{cc}}{D}b_0-b_1\mu=0,$$

$$2c_2\mu=0,\ \ k_0c_2+c_1\mu=0,\ \ k_0c_1-2c_2\mu=0,\ \ k_0c_0-c_1\mu=0.$$

Solving the system (24), we obtain the parameters $a_2, b_0, b_1, b_2, b_3, c_0, c_1,$ and c_2 expressed in terms a_0, a_1 as follows:

$$a_2=-\frac{v+k_{cc}}{2\mu D}a_1-3a_0,$$

$$b_0=\mu a_1,\ \ b_1=-\frac{v+k_{cc}}{D}a_1-6\mu a_0,\ b_2=-\mu a_1,\ b_3=\frac{v+k_{cc}}{D}a_1+6\mu a_0, \tag{25}$$

$$c_0=-\frac{6\mu^2D}{\alpha},\ c_1=0,\ \ c_2=\frac{6\mu^2D}{\alpha}.$$

Thus, we obtain the following analytical solution for the level of carbohydrates in the intestine.

$$C(t,z)=a_0+a_1\tanh\left(\mu(z-vt)\right)-\left(\frac{v+k_{cc}}{2\mu D}a_1+3a_0\right)\tanh^2\left(\mu(z-vt)\right) \tag{28}$$

RESULTS

With the help of the equations in (25), once we fix the values of a_0 and a_2, the values of the remaining coefficients are automatically set. Then, the coefficient values obtained in this manner can be substituted into the expression for the carbohydrate content (28), the plot of which, seen in Fig.1, provides us with the view of the wave front of consumed carbohydrates traveling through space and time.

International Journal of Environmental Sciences
ISSN: 2229-7359
Vol. 11 No.9s, 2025
https://www.theaspd.com/ijes.php

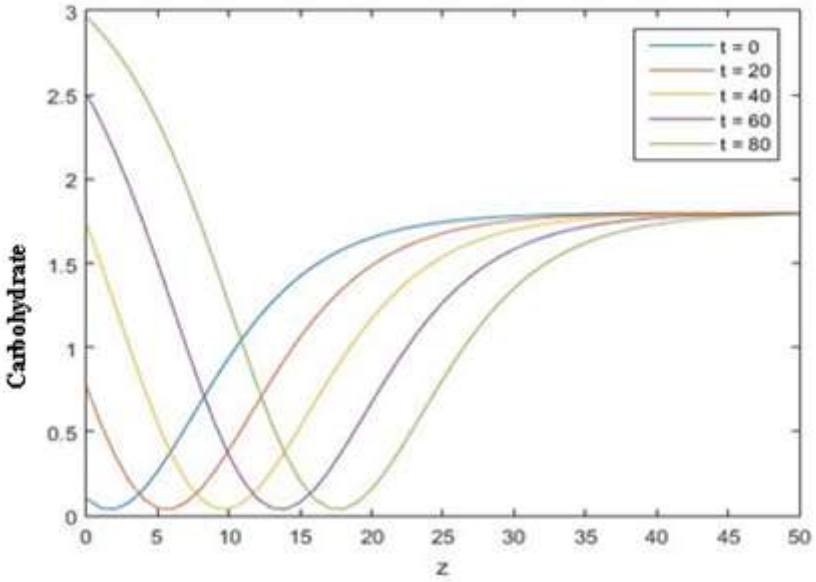

Figure 1. Traveling wave of C, the digested carbohydrate for different time and spatial distance *z*.

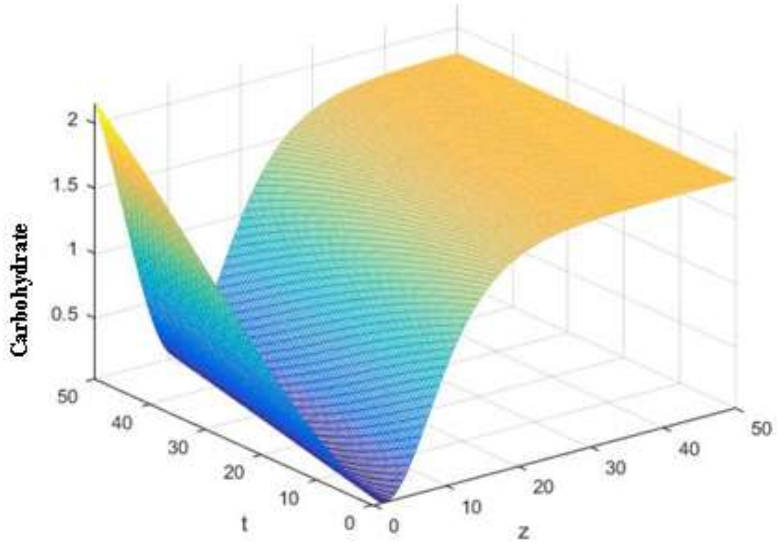

Figure 2. Three dimensional plot of C(*t*, *z*) as a function of space *z* and time *t*.

Fig. 1 above shows the analytical solution for C(*t*, *z*), plotted as wave fronts traveling through time *t*, here ranging from 0 to 80, along the length of the small intestine which may be assumed to be very long. Here, $a_0 = 0.1$, $a_1 = -0.8$, $a_2 = 2.5$, $b_0 =$, $b_1 =$, $b_2 =$, $b_3 = c_0 =$, $c_1 =$, $c_2 =$, $\alpha = 0.1$, D = 1.0, v = 0.2, K_{CC} = 0.5, k_0 = 0.1, $\mu = 0.1$. Figure2 shows the corresponding three dimensional plot of C(*t*, *z*) as a function of space *z* and time *t*, by which we may easily identify the level of digested carbohydrate remaining in the small intestine at any moment in time and at any spatial location along the intestinal tract.

Glucose and Insulin Time Series

It is now possible to derive the levels of glucose and insulin by numerically simulating the following system.

$$\frac{dG}{dt} = R_0 + \alpha\tilde{C} - GS_I \frac{I}{I_{GS_0} + I}, \tag{29}$$

$$\frac{dI}{dt} = \sigma^{\max} \frac{G^{\sigma_{IG}}}{G_{IS_0}^{\sigma_{IG}} + G^{\sigma_{IG}}} - k_{0I} I \tag{30}$$

$$\frac{dK_0}{dt} = -vk_0 K_0 \tag{31}$$

$$\frac{d\tilde{C}}{dt} = \gamma(t)K(t) + \beta\tilde{C}(t) \tag{32}$$

where (29) is the rate of change of glucose from equation (2), and (30) is the rate of change of insulin from equation (3). To simplify our simulation, we have introduced the new variables:

$$\tilde{C}(t) = \int_0^l \kappa C(t,z)dz, \tag{33}$$

and

$$K_0 = e^{k_0(z-vt)}, \tag{34}$$

in which the analytical solution for C(*t*, *z*) is now known, expressible as in (28). The above integral in (33) can be done since we already know the explicit formula for C(*t*, *z*) whose graph is seen in Fig. 1, where it can be observed that, as *z* becomes very large, C(*t*, *z*) tends asymptotically to a constant level. Therefore, at the far end of the very long digestive tract, we may assume that

$$\left.\frac{\partial C}{\partial z}\right|_{z=l} = 0.$$

Thus, we are able to find that, in (32),

$$\gamma(t) = (k_0 D - k_{CC})\left(C(t,0) - e^{k_0}\right) - D\frac{\partial C}{\partial z}(t,0),$$

and

$$\beta = k_0^2 D - k_0 k_{CC} - vk_0 - 1.$$

The parametric values used in our simulations have been taken partly from the work by Barbiero and Lió on the computational patient with diabetes and A COVID [4], and the seminal work by **De Gaetano et al. on** mathematical models of diabetes progression [5], are provided in Table 1 below. Table 2 provides the values the coefficients in the expansions (21) – (23), satisfying the relationships in (25), which have been derived through the use of traveling wave coordinate and the modified extended hyperbolic tangent method described by Taghizadeh, and Mirzazadeh in [6], resulting in the graphs of C(*t*, *z*) shown in Fig. 1 and Fig. 2.

The resulting time series for G(*t*), *I*(*t*), $K_0(t)$, and $\tilde{C}(t)$, are shown in Fig. 3A through 3D, respectively.

Table 1: Parametric values used in numerical simulation of (29) – (32) with (33).

Parameter	Value	Source
R_0	1.0864 $ml\ dl^{-1}g^{-1}$	[4]
S_I	0.1	[4]
I_{GS_0}	0.359	[4]
σ_{IG}	2	[5]

$\sigma_{\max}$	0.176134 $\mu U\ ml^{-1}d^{-1}$	[4]
G_{IS_0}	0.02 ml^2dl^{-2}	[4]
k_{0I}	0.432 d^{-1}	[4]

Table 2: Coefficients in the expansions (21) – (23) used in (33)

Parameter	Value	Parameter	Value	Parameter	Value
α	0.1	k_0	0.1	k_{CC}	0.5
μ	0.2	v	0.2	D	1
a_0	0.1	b_0	-0.08	c_0	-0.6
a_1	1.0	b_1	0.5	c_1	0.0
a_2	-1.05	b_2	0.08	c_2	0.6
		b_3	-0.5		

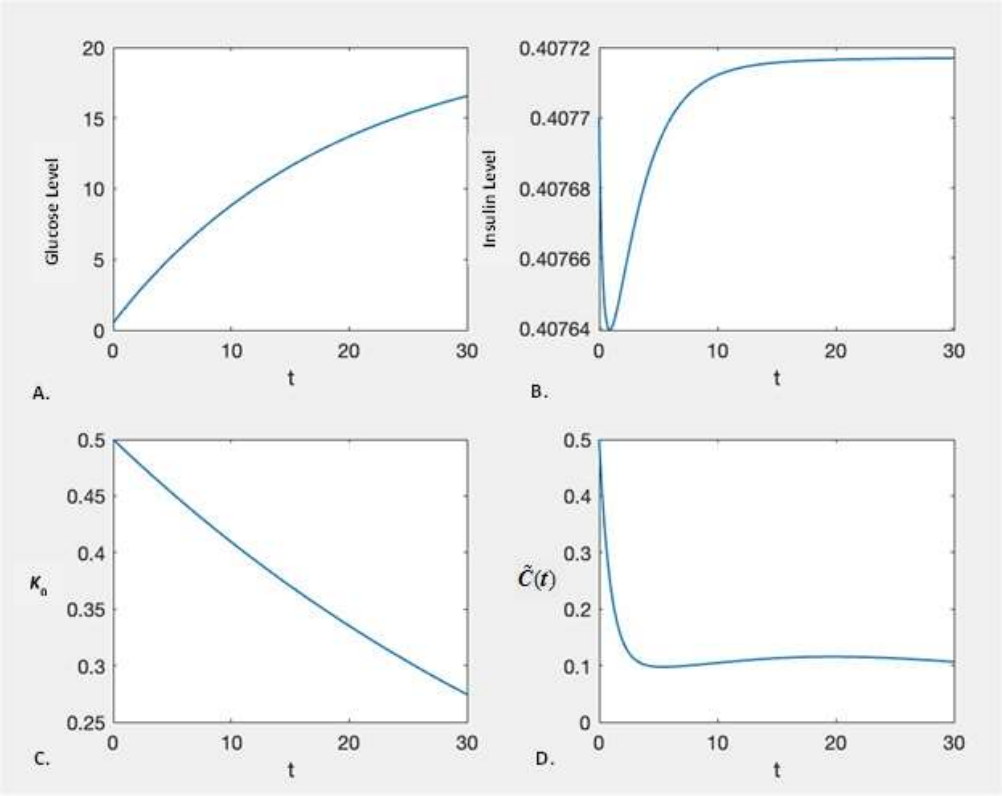

Figure 3. Time series of A. G(t), B. $I(t)$, C. $K_0(t)$, and D. $\tilde{C}(t)$.

DISCUSSION

When the parameters in the model system are adjusted to fit different physiological types, we may begin to understand the different impacts of high or low carbohydrate food intakes. For example, v reflects how fast the consumed food travels thru a person's intestine while carbohydrate is absorbed. κ and k_0 reflect the gastric absorption efficiency of each person. The parameters $\sigma^{\max}$ and $G_{IS_0}^{\sigma_{IG}}$ reflect how the body reacts to an increase in glucose and how fast it saturates. When one parameter is high, while the other is low, the reaction could be much different in a person with the reverse being true.

By varying these parameters, we may determine how food digestion with initial carbohydrate content $C(0,t)$, and initial glucose level in the person bloodstream, will affect the person's glucose-insulin control system at different times and locations.

As an example, let's considering Fig. 1 more closely. What we've shown here is the case in which

initially (t = 0 along the blue curve) the carbohydrate content is close to 0 at the start of the digestive tract (z = 0), meaning not much carbohydrate remains around this point to begin with. However, a distance from the beginning of the tract, far to the right of the axis, a finite amount of carbohydrates still remains, tending asymptotically to a constant value. As time progress, we can see that the curve moves from left to right. If we keep our attention on a fixed position $z = z_0$ □ 1 along the tract, we see that the carbohydrate starts to rise, from the level on the blue curve to orange to yellow, then to the green level. On the other hand, if we are further along the digestive tract, the carbohydrate level will fall since the digested food has not reach that point yet, until the time has sufficiently passed, at which point the carbohydrate will begin to rise. Now, with different values of κ, k_0, $\sigma^{\max}$ or $G_{IS_0}^{\sigma_{IG}}$, for example, the levels will vary in a dynamically different manner, modelling a different person of different physiological type.

Furthermore, from the exact solution of $C(t, z)$, we can simulate the system model for the time series of glucose and insulin levels for a particular physiological type, as a result of the types of nutritional contents being consumed. The graphs shown in Fig. 4, were obtained for initial conditions that $G(0) = 0.5$ and $I(0) = 0.4077$. We see that in this case, it is felt by the control mechanism that the level of glucose in the bloodstream is still not too high, and so the amount of insulin initially decreases. However, as the carbohydrates are absorbed and converted to more glucose in the bloodstream, the pancreas is triggered to secrete insulin to try to bring the glucose level to a constant level. However, in the case shown, the digested carbohydrates continue to be absorbed and thus the glucose level is expected to continue to increase, escaping insulin's control. This scenario appears to be the case where a supplementary insulin injection might be called for.

CONCLUSION

We have constructed a three compartmental dynamical model of the glucose-insulin control system which incorporates the process of carbohydrate absorption in the small intestine. The cross-membrane absorption process was described with the use of an exponential function so that the amount absorbed per unit of digested carbohydrate varies with space and time. Consequently, the rate of change of the amount of carbohydrates has been modeled by a partial differential equation. Our model thus consisted of a system of integro-differential non-autonomous equations.

New state variables which vary with the traveling wave coordinate led us to a system of ordinary differential equations. After carrying out a stability analysis, an analytical solution has been obtained in the form of a wave solution traveling along the length of the digestive tract. Time series of both glucose and insulin levels as functions of time have been illustrated to be useful for us to predict the impacts of high or low starch content in our food intake on the glucose-insulin control system for diabetics or healthy subjects, so that appropriate actions could be taken to mediate the effects of high or low starch content in our food intake.

From the above discussion, it is apparent that our effort at modeling and deriving analytical solutions can become a valuable tool in our drive towards personalized medicine [11], also known as precision medicine, which has the objective of tailoring healthcare to fit individual patients [12] by taking into account their unique genetic factors, environments, and lifestyles, bringing about more effective and safer treatments.

ACKNOWLEDGEMENTS

The authors would like to thank Dr. Andrea de Gaetano of the BioMathematics Lab, CNR IASI, Rome, Italy, and Dr. Permyos Ruengsakulrach, MD, of the Bangkok Heart Hospital, Thailand, for their valuable advice and insightful suggestions. Appreciations are also extended towards the Centre of Excellence in Mathematics, PERDO, MHESI, for the financial support that has made this research possible.

REFERENCES

[1]. Julie E. Holesh; Sanah Aslam; Andrew Martin, 2023, Physiology, Carbohydrates. National Library of Medicine, National Center for Biotechnology Information (Treasure Island (FL): StatPearls Publishing).

[2]. Bolla, A. M., Caretto, A., Laurenzi, A., Scavini, M., Piemonti, L., 2019, Low-Carb and ketogenic diets in type 1 and type 2 diabetes. *Nutrients*. 11(5), 962, doi: 10.3390/nu11050962.

[3]. Mills, S., Stanton, C., Lane, J. A., Smith, G. J., Ross, R. P., 2019, Precision nutrition and the microbiome, part I: current state of the science. *Nutrients*. 11(4), 923, DOI: 10.3390/nu11040923.

[4]. Barbiero, P., Lió, P., 2020, The computational patient has diabetes and A COVID, *medRxiv*. doi: https://doi.org/10.1101/2020.06.10.20127183.

[5]. **De Gaetano, A., Hardy, T., Beck, B., Abu-Raddad, E., Palumbo, P., Bue-Valleskey, J., Pørksen, N., 2008,** Mathematical models of diabetes progression. *Am J Physiol Endocrinol Metab*. **295: E1462–E1479.**

[6]. Taghizadeh, N., Mirzazadeh, M., 2012, The Modified Extended Tanh method with the Riccati equation for solving nonlinear partial differential equations, *Math. Æterna*. 2(2), 145-153.

[7]. Suksamran, J., Lenbury, Y., Satiracoo, P., Rattanakul, C., 2017, A model for Porcine Reproductive and Respiratory Syndrome with timedependent infection rate: traveling wave solution, ***Advances in Difference Equations***. 215, 1-11.

[8]. Abdou, M. A., 2007, The extended tanh method and its applications for solving nonlinear nonlinear physical models, ***Appl. Math. Comput.*** 190(1), 988-996.

[9]. Zedan, H. A., New approach for tanh and extended-tanh methods with applications on Hirota-Satsuma equations, ***Comput. Appl. Math.***, vol. 28(1), 1-14.

[10]. Suksamran, J., Amornsamankul, S., Lenbury, Y., 2024, Reaction-diffusion-integral system modeling SARS-CoV-2 infection-induced versus vaccine-induced immunity: analytical solutions and stability analysis, *IAENG International Journal of Applied Mathematics*. 54(2), 223-231.

[11]. Goetz, L. H., Schork, N. J., 2018, Personalized Medicine: Motivation, Challenges and Progress, Fertil Steril. 109(6):952–963.

[12]. Kong, D., Yu, H., Sim, X., White, K., Tai, E. S., Wenk, M., Teo, A. K. K., 2022, Multidisciplinary effort to drive precision-medicine for the future, *Front. Digit. Health*. 4 – 2022, https://doi.org/10.3389/fdgth.2022.845405.